Journal of Alloys and Compounds 509 (2011) 6556–6560

Contents lists available at ScienceDirect

Journal of Alloys and Compounds

journal homepage: www.elsevier.com/locate/jallcom

Structurally modulated precipitates in a refractory Cr–V alloy

Ömer N. Doğan[a,*], Song Chen[b], Xueyan Song[b], John Sears[c]

[a] National Energy Technology Laboratory, 1450 Queen Ave., S.W., Albany, OR 97321, USA
[b] Department of Mechanical and Aerospace Engineering, West Virginia University, Morgantown, WV 26506, USA
[c] URS, P.O. Box 1959, Albany, OR 97321, USA

ARTICLE INFO

Article history:
Received 23 December 2010
Received in revised form 22 March 2011
Accepted 25 March 2011
Available online 1 April 2011

Keywords:
High-temperature alloys
Transition metal alloys and compounds
Crystal structure
Transmission electron microscopy (TEM)

ABSTRACT

Chromium alloys are considered as high temperature structural materials. Vanadium was substitutionally alloyed into chromium to improve its room temperature ductility. Precipitates, which were indexed as $C_{20}Cr_{25}V_{55}$ with an orthorombic structure, form in these chromium–vanadium alloys due to the presence of carbon impurities. The distribution, morphology, and crystal defects of the precipitates were studied using electron diffraction, diffraction contrast imaging, and high resolution transmission electron microscopy. One-dimensional structural modulations were determined in these precipitates.

Published by Elsevier B.V.

1. Introduction

Fossil fuels will be used as a major energy source in the foreseeable future. Clean energy conversion technologies such as hydrogen turbines and oxyfuel turbines are being developed to utilize these fossil fuels without harmful emissions. Because these more efficient turbines will operate at significantly higher temperatures than today's gas turbines, lack of appropriate structural and functional materials constitutes one of the largest barriers to the realization of these new technologies. Today, gas turbine structural components such as blades are constructed using Ni-based superalloys that are the most advanced materials available for this application. However, these components in the new turbines will be exposed to significantly higher temperatures (inlet temperatures up to 1750 °C). Although utilizing cooling strategies and coatings will reduce the temperature that the component substrate will experience, still these temperatures will be beyond the capability of the Ni-based superalloys. Therefore, there is an urgent need to develop new structural materials that are capable of operating in the extreme conditions.

Alloys of body-centered cubic (bcc) refractory metals with high melting points [1–3] are promising candidate materials for these structural applications. In particular, chromium alloys are attractive because they have low density, high thermal conductivity, and high strength at elevated temperatures. Chromium generally forms a dense surface scale of Cr_2O_3 that possesses excellent corrosion resistance at high temperatures (≤900–1100 °C depending on oxygen partial pressure). In addition, strategies have been developed for the Cr alloys to maintain acceptable oxidation resistance at higher temperatures (≥1000 °C) [4]. More importantly, Cr is inexpensive compared to the other refractory metals because it is more abundant. However, its low-temperature (e.g., room temperature) brittleness has precluded it from major engineering applications [5]. Recently, it has been suggested that alloying with certain substitutional elements can improve the ductility of chromium [6]. Vanadium was found to be one of the most effective "ductilizers". Alloying chromium with vanadium introduces high levels of carbon impurity into the alloy because commercially available vanadium contains 0.1–0.2 weight percent carbon due to the reduction process used to produce it. In this report, microstructural characterization of a chromium–vanadium alloy is presented. The effect of carbon impurity on the microstructure of the Cr–V alloy is discussed in detail.

2. Experimental

A Cr–V alloy (approximately 400 g) containing nominally 50% V was synthesized on a water-cooled copper hearth in a vacuum arc furnace. The alloy was remelted three times to ensure homogeneity. Elemental Cr (99.95 wt.% purity) and V (99.7 wt.% purity) flakes were used as charge materials. A heat treatment was performed to further homogenize the distribution of elements that segregated during solidification. The heat treatment was done in a vacuum furnace back-filled with high purity argon, at 1200 °C for 8 h. The chemical composition of the alloy was analyzed using X-ray fluorescence (XRF) and a gas analysis technique (Table 1). Yttrium was added to tie the interstitials that were introduced with the raw materials. A significant amount of boron was also detected. However, the reason for B detection and its origin are unknown.

* Corresponding author. Tel.: +1 541 967 5858; fax: +1 541 918 8090.
E-mail address: omer.dogan@netl.doe.gov (Ö.N. Doğan).

0925-8388/$ – see front matter. Published by Elsevier B.V.
doi:10.1016/j.jallcom.2011.03.146

Table 1
Composition (wt.%) of the investigated alloy.

Cr	V	Y	N	O	S	C	B	Al	Si	Fe	Mo
Bal.	49.14	0.31	0.004	0.004	0.0009	0.06	0.63	0.023	0.023	0.052	0.067

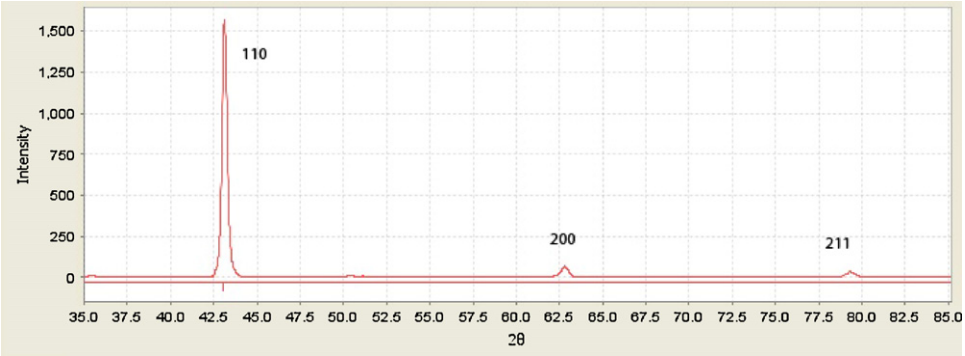

Fig. 1. XRD pattern obtained from the Cr–V alloy investigated in this study.

X-ray diffraction (XRD) analysis was performed using a Rigaku Ultima III instrument utilizing Cu-K_α radiation. Scanning electron microscopy (SEM) and transmission electron microscopy (TEM) were employed to characterize the microstructure. TEM samples were prepared by mechanical polishing and ion milling, where the TEM samples were cooled using liquid nitrogen during the ion-milling process. Diffraction contrast imaging, electron diffraction, high resolution TEM imaging and microchemical analysis were performed in a JEOL 2100 and Philips CM200, both equipped with a LaB_6 electron source and X-ray Energy Dispersive Spectrometry (XEDS).

3. Results and discussion

The XRD pattern from the Cr–V alloy, with the composition detailed in Table 1, is shown in Fig. 1. From the XRD pattern, it can be determined that the present alloy has a bcc crystal structure with a lattice parameter of 2.957 Å. This lattice parameter of the Cr–V bcc alloy in agreement with data reported in literature [7].

SEM results demonstrated that the Cr–V alloy is comprised of a solid solution matrix phase and various second phase particles. The matrix phase has large grains of 30–100 μm and most of the large second phase particles are located on the few grain boundaries. The large second phase particles seen in Fig. 2 are as a result of the intentional addition of yttrium for tying the interstitial impurity elements. They are primarily yttrium oxide and yttrium sulfide particles with the size of 0.5–1 μm as evidenced from EDS results of SEM and TEM analysis. Although significant concentration of boron was detected by XRF during the general compositional analysis of the sample, no compounds containing high concentrations of boron

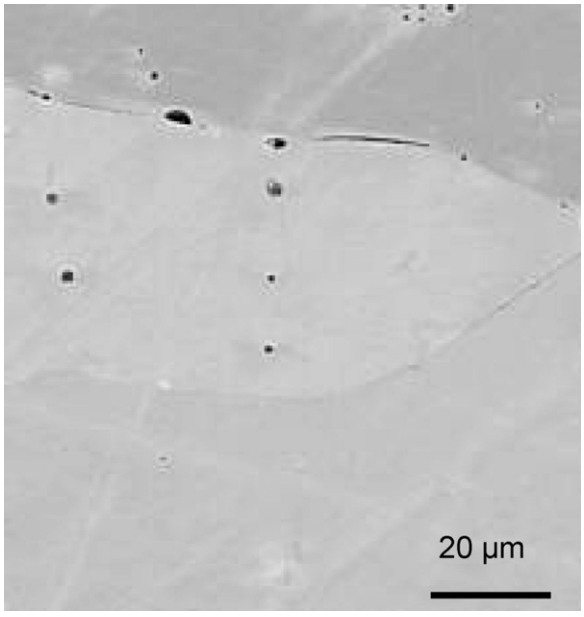

Fig. 2. Back-scattered electron image of the microstructure of the experimental alloy.

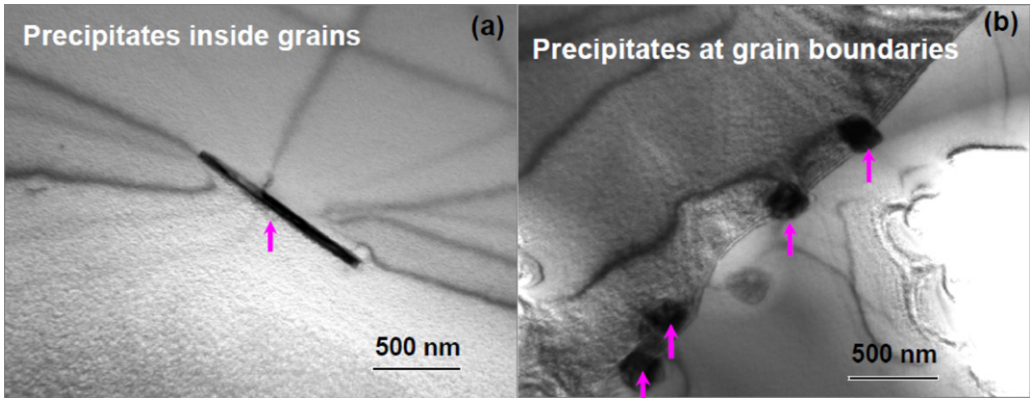

Fig. 3. TEM bright field images of intragranular (a) and intergranular (b) precipitates.

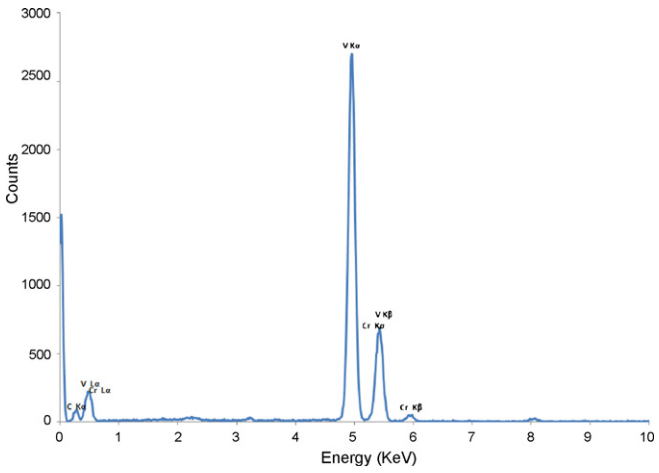

Fig. 4. TEM-EDS results of the precipitates shown in Fig. 3.

was observed in the microstructure. It is possible that boron segregates to the grain boundaries and precipitate-matrix interfaces although no evidence was collected in this material to support this hypothesis.

In addition to the large scale spherical particles shown in Fig. 2, TEM diffraction contrast images show the existence of needle shaped precipitates with the aspect ratio of 10:1 (i.e., long axis of 1 μm and shorter axis of ~100 nm). Those needle shaped precipitates are randomly dispersed inside the Cr-alloy grains, as shown in Fig. 3(a). On the other hand, intergranular, square shaped precipitates with a dimension of ~150 nm are observed as shown in Fig. 3(b). The EDS results in Fig. 4 indicate that both the intragranular precipitate and intergranular square shaped precipitates are composed of Cr, V, and C. The atomic ratio is about C:Cr:V of 10:10:80.

The electron diffraction originating from both the intergranular and intragranular precipitates yields the same pattern, shown in Fig. 5. Selected area diffraction patterns (SADP) were obtained from the precipitates without contribution from the matrix. This is a complex diffraction pattern with the primary spots accompanied by a series of additional spots.

The diffraction symmetry and calculated interplanar spacing for the primary diffraction spots from the precipitates matched that from the $C_{20}Cr_{25}V_{55}$ in the C–Cr–V system found in the database [8], even though the overall composition of the precipitates, as determined by XEDS, is off from that of $C_{20}Cr_{25}V_{55}$. This $C_{20}Cr_{25}V_{55}$ phase has an orthorhombic structure with lattice parameters of $a = 4.530$ Å, $b = 5.736$ Å, and $c = 5.012$ Å. The diffraction pattern shown in Fig. 5 is thus indexed as the [0 1 0] zone axis of $C_{20}Cr_{25}V_{55}$.

Note that the $C_{20}Cr_{25}V_{55}$ phase is indexed based on the primary diffraction spots, indicated in Fig. 5 by the arrows. In addition to the primary diffraction spots, additional diffraction spots of type (1 0 0) for the $C_{20}Cr_{25}V_{55}$ phase, and satellite spots for each of the primary diffraction spots are apparent. These additional spots and the weak diffraction spots close to the primary diffraction spots from the basic structure reveal the existence of modulated structure for this phase. In general, a modulated phase usually contains several types of units, each type undergoing a different modulation. We thus treat the diffraction pattern in Fig. 5 as the superposition of the corresponding diffraction from each unit.

In the present study, the atomic resolution HRTEM images and Fourier and inverse Fourier transformations are used to deduce the superposition of diffraction from different units in the $C_{20}Cr_{25}V_{55}$ phase. Systematic imaging analysis indicates that these two types of additional diffraction spots are as a result of modulations shown in Fig. 6. The first modulation creates spots that can be considered as new Bragg diffractions (kinematically forbidden diffraction)

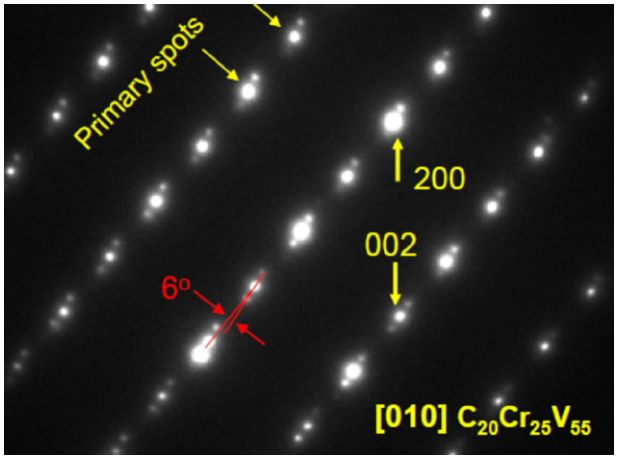

Fig. 5. SADP taken from the grain boundary precipitates in Fig. 3.

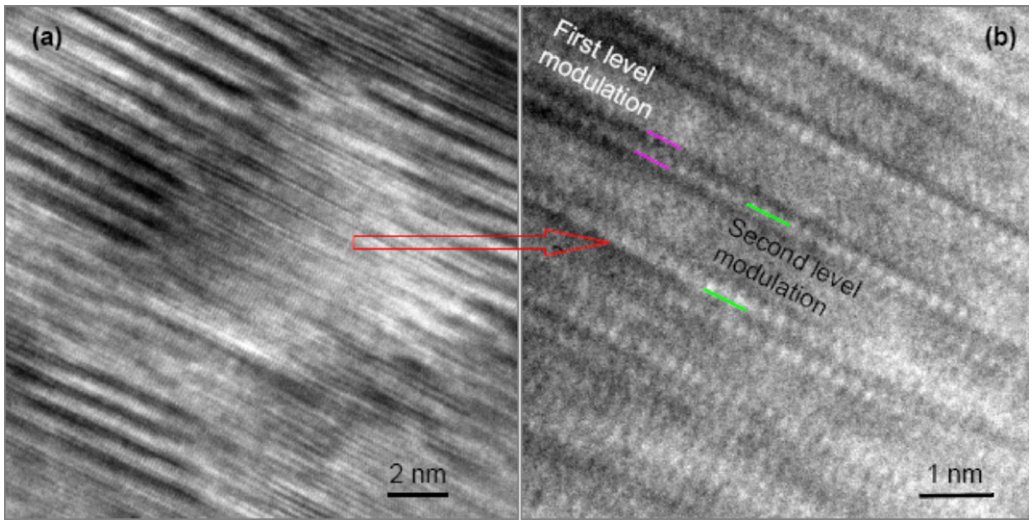

Fig. 6. HRTEM images showing the two modulations in the $C_{20}Cr_{25}V_{55}$ precipitates.

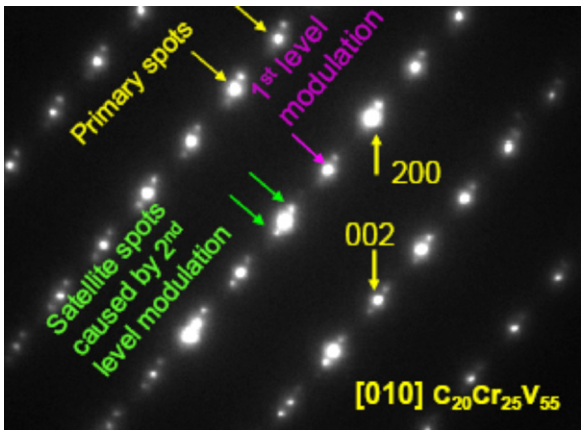

Fig. 7. Diffraction pattern indicating the spots that correspond to the first and second level of modulations.

in one dimension [1 0 0] for the orthorombic phase as shown in Fig. 7. These spots are from the first level of modulation indicated in HRTEM images in Fig. 6. In addition, the satellite spots are originated from the second level of modulation, again in one dimension as shown in Fig. 7. The structure of the second level of modulations is also shown in Fig. 6.

HRTEM images reveal that these modulations are not uniform throughout the orthorhombic phase. A modulated structure usually originates from a basic structure, which contains entities that can be altered, located on a perfectly periodic lattice. The modulation then consists of the modification of these entities by one or more driving forces such as chemistry changes, which tend to impose their periodicities that need not be the same as those of the basic lattice. If this periodicity is not rationally related in spacing and/or orientation to the basic periodicity, the modulation is called incommensurate [9]. As shown in Fig. 5, the one-dimensional satellite spots possess a rotation angle of ~6° relative to the primary spots and thus the present modulation is incommensurate.

In addition to the one-dimensional modulations, HRTEM images also reveal the presence of "islands" with different crystal structure included in the orthorhombic phase as shown in Fig. 8. The Fourier transformation from this structure clearly show that these "islands" possess a fcc structure as shown in the diffraction pattern with the zone axis of [0 1 1] in Fig. 8(d). The fcc phase has a lattice parameter of approximately 4 Å which is close to that of the $Cr_{20}V_{30}C_{50}$ phase (4.132 Å) in the database 8]. The indexed $C_{20}Cr_{25}V_{55}$ orthorombic phase and the island fcc phase are with the orientation relationship of $[0\,1\,0]_{orth}//[0\,1\,1]_{fcc}$ and $(2\,0\,0)_{orth}//(11{-}1)_{fcc}$.

These "islands" are possibly the basic structure of the $C_{20}Cr_{25}V_{55}$ orthorombic phase with modulation and the indexed $C_{20}Cr_{25}V_{55}$ orthorombic phase can be treated as a variant of the $Cr_{20}V_{30}C_{50}$ fcc phase. It is very likely that the island-like fcc structure has a different composition from that of the modulated region. Because the dimension of the region with the fcc structure is around 5 nm, the composition of the basic structure is not identified in the JEM-2100 microscope equipped with a LaB_6 filament. The presence of island regions and the possible compositional variations within the precipitates may be the cause of the discrepancy between the composition obtained from the XEDS spectrum shown in Fig. 4 and that of the indexed $C_{20}Cr_{25}V_{55}$ orthorhombic phase.

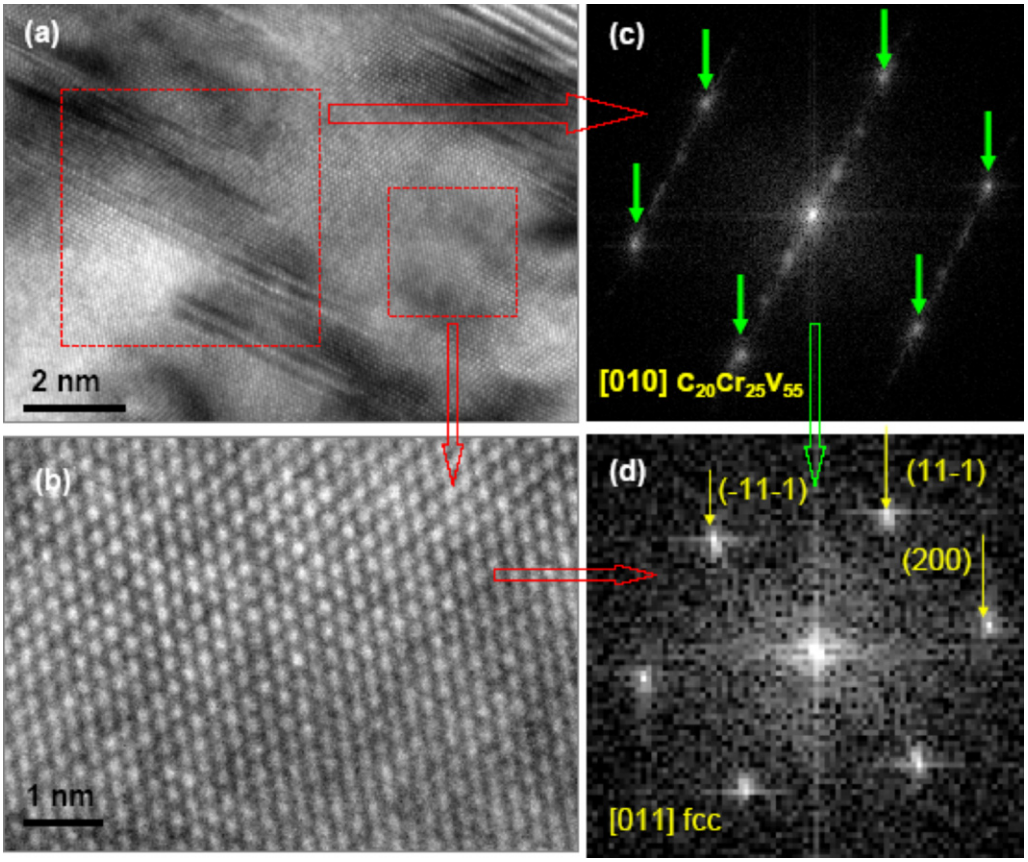

Fig. 8. HRTEM image showing the first and second level modulations as well as the fcc structure in the orthorhombic $C_{20}Cr_{25}V_{55}$. (a) HRTEM image taken from C–Cr–V phase, (b) Magnified image of the smaller framed area in (a), (c) Fourier transformation of the larger framed area in (a), and (d) Fourier transformation of the imaged area in (b).

The effect of Cr–V–C precipitates on the mechanical properties of the Cr–V alloys is unclear at this point. However, since these alloys are envisioned for high temperature applications, it is possible that the newly discovered precipitates can be utilized as creep strengtheners.

4. Conclusions

Detailed microstructure analysis was carried out on a refractory Cr–V alloy. Results show that the Cr–V alloy is comprised of a solid solution matrix phase and various second phase particles. Precipitates that are indexed as $C_{20}Cr_{25}V_{55}$ with an orthorhombic crystal structure were identified in both the grain interior and grain boundaries of the Cr–V solid solution with bcc structure. One-dimensional structural modulations were determined in these precipitates using high resolution TEM.

Acknowledgements

This research was performed in support of the Advanced Research Program of the NETL's Strategic Center for Coal.

References

[1] B.P. Bewlay, M.R. Jackson, J.C. Zhao, P.R. Subramanian, Metallurgical and Materials Transactions A: Physical Metallurgy and Materials Science 34A (2003) 2043–2052.
[2] G. Ghosh, G.B. Olson, Acta Materialia 55 (2007) 3281–3303.
[3] R. Sakidja, J.H. Perepezko, Journal of Nuclear Materials 366 (2007) 407–416.
[4] Ö.N. Doğan, Oxidation of Metals 69 (2008) 233–247.
[5] W.D. Klopp, Journal of the Less Common Metals 42 (1975) 261–278.
[6] M.C Gao, Ö.N. Doğan, P. King, A.D. Rollett, M. Widom, JOM 60 (2008) 61–65.
[7] W.B. Pearson, A Handbook of Lattice Spacings and Structures of Metals and Alloys, Pergamon Press, 1967.
[8] PDF-4, International Center for Diffraction Data (2009).
[9] J.M. Cowley, Electron Diffraction Techniques, International Union of Crystallography, Oxford Science Publications, 1992.